Published in final edited form as:
Dev Cell. 2014 May 12; 29(3): 350–359. doi:10.1016/j.devcel.2014.04.003.

A Pak1/Erk Signaling Module Acts through Gata6 to Regulate Cardiovascular Development in Zebrafish

Mollie L. Kelly[1,2], **Artyom Astsaturov**[1], **Jennifer Rhodes**[1], and **Jonathan Chernoff**[1]

[1]Cancer Biology Program, Fox Chase Cancer Center, Philadelphia, PA

[2]Department of Biochemistry and Molecular Biology, Drexel University, Philadelphia, PA

Summary

Proper neural crest development and migration is critical during embryonic development, but the molecular mechanisms regulating this process remain incompletely understood. Here, we show that the protein kinase Erk, which plays a central role in a number of key developmental processes in vertebrates, is regulated in the developing neural crest by p21-activated protein kinase-1 (Pak1). Further, we show that activated Erk signals by phosphorylating the transcription factor Gata6 on a conserved serine residue to promote neural crest migration and proper formation of craniofacial structures, pigment cells, and the outflow tract of the heart. Our data suggest a previously unrecognized and essential role for Pak1 as an Erk activator, and Gata6 as an Erk target, during neural crest development.

Keywords

Zebrafish development; protein kinases; p21-activated kinase; Erk; Gata6; small GTPases; signal transduction

Introduction

The Erk signaling pathway is central to a number of cellular processes such as transcription, cell proliferation, and differentiation (Krens et al., 2008). (Krens et al., 2008). Erks have been shown to mediate cell migration during gastrulation of zebrafish embryos (Krens et al., 2008). In addition, pharmacologic inhibition of the Erk activator Mek in zebrafish results in defective cranio-facial development, outflow tract blockage in the heart with concomitant pericardial edema, and increased vascular permeability (Anastasaki et al., 2012; Bolcome and Chan, 2010). Conversely, overactivation of Erk by expression of constitutive active Shp2, Sos, Ras, Raf, or Mek mutants, is also associated with a variety of heart defects in zebrafish (Jopling et al., 2007; Razzaque et al., 2012; Runtuwene et al., 2011; Stewart et al.,

To whom correspondence should be addressed: Jonathan Chernoff, Cancer Biology Program, Fox Chase Cancer Center, 333 Cottman Ave, Philadelphia, PA 19111, USA, Tel.: (215) 728 5319; Fax: (215) 728 3616; Jonathan.Chernoff@fccc.edu.

2010). Despite its central role, the identity of upstream activators of Erk, and its downstream targets that regulate developmental pathways, are poorly understood.

p21-activated kinase1 (Pak1) is a serine/threonine kinase that acts downstream of the small GTPases Cdc42 and Rac1 to regulate a multitude of cellular processes including transcription, translation, cell motility, survival, proliferation, and organization of the cytoskeleton (Arias-Romero and Chernoff, 2008). Some of the functions of Pak1 are related to its ability to serve as a scaffold protein (Higuchi et al., 2008); however the bulk of its activities are believed to be due to its ability to phosphorylate various targets (Bokoch, 2003; Dummler et al., 2009). Among the most firmly established substrates of Pak1 are c-Raf and Mek1, and we and others have shown that loss of Pak1 activity leads to loss of c-Raf, Mek1, and subsequent Erk activation in many cell types (Arias-Romero and Chernoff, 2008). While Pak1 also has many other substrates besides c-Raf and Mek1 that mediate its cellular effects, recent genetic and pharmacologic data show that the Pak/Mek/Erk signaling axis is essential for transformation in a K-ras-driven mouse model of skin cancer (Chow et al., 2012).

Here, we report that knockdown of Pak1 in zebrafish embryos causes defects in neural crest development, characterized by a linear heart tube and outflow tract blockage, impaired melanophore development and migration, and aberrant cartilage structure. These developmental defects are accompanied by loss of Erk activity, and can be suppressed by expression of activated Mek1 or by a phospho-mimic form of an Erk substrate, the transcription factor Gata6. These results establish a molecular signaling pathway from Pak1 to Mek/Erk to Gata6 that is required for proper development of the neural crest.

Results

Pak1 Expression in Zebrafish

To examine the expression pattern of *pak1* in zebrafish, we performed a whole mount *in situ* hybridization throughout development. *Pak1* expression was ubiquitous at the one-cell stage through 100% epiboly (Figure 1A). By 24 hours post fertilization (hpf), *pak1* was expressed in low levels throughout the embryo with more prominent expression in the central nervous system and intersomitic vessels. By 48 hpf, *pak1* expression was easily detected in the central nervous system, and weakly detected in the intersomitic vessels and heart. To further demonstrate expression, we used reverse transcriptase PCR to detect *pak1* expression at multiple developmental stages. This experiment revealed that *pak1* was expressed from the one-cell stage to 72 hpf (Figure 1B).

Knockdown and Rescue of pak1 in the Developing Zebrafish

To determine the contribution of *pak1* to development, we designed a morpholino (MO) against the intron/exon splice site of *pak1* and injected this MO at the one-cell stage. Both RT-PCR and immunoblot showed the MO was effective at knocking down *pak1* through 48 hpf (Figure 1C and 1D). The MO was then titrated to determine the minimal doses needed to give reliable phenotypes (Figure S1A-B and Table S1). Control MOs, containing mismatches to the *pak1* target sequence (MM), had no effect on *pak1* mRNA or protein

expression (Figure 1C and 1D). In addition, we tested ATG MOs against *pak1* and splice site MOs against both *pak2a* and *pak2b*. The *pak1* ATG MO injected morphants showed a phenotype similar to that of the *pak1* splice site MO. In contrast, *pak2a* MO showed hemorrhaging in the head while *pak2b* MO displayed no observable phenotype, similar to published reports (Figure S1C and Table S2) (Buchner et al., 2007).

At 24 hpf, the vast majority of *pak1* morphants displayed one of two phenotypes – moderate (78%) or severe (18%) - with the moderate phenotype consisting of significant developmental defects including a general loss of tissue, cell death in the head, a curled body axis, and pericardial edema (Figure 1E and 1F and Table S1). These phenotypes were also observed at 48 hpf, with gross morphological defects in the heart, along with no/slowed circulation (Figure 1E). Such moderate morphants had normal heart rates, indicating a lack of gross conductance defects (data not shown). A small percentage of severe *pak1* morphants displayed a significant loss of tissue, cell death, and loss of circulation (Figure 1E).

The severe *pak1* morphants displayed an extensive loss of tissue throughout the body with an enhanced cell death through the head region compared to WT embryos and control MO injected embryos (Figure 1E and S1E). These effects were also seen in *p53*-null embryos injected with *pak1* MOs, indicating that the tissue loss was not secondary to a general p53-mediated apoptosis induced by *pak1* MO injection (Figure S1F).

As the *pak1* morphant phenotype was so striking at 24 hpf, we assessed the patterning of the embryo during gastrulation and tissue specification. Convergence-extension (CE) movements were not notably perturbed by *pak1* MOs, with a normal body axis ratio and normal bilateral staining of *hgg1* and *dlx3* markers at 10 hpf (Figure S1I). The expression and distribution of *bone morphogenetic protein 4* (*bmp4*), which is involved in the specification of ventral cell fates, was not affected by knockdown of *pak1* (Figure S1J). Similarly, expression of the dorsal specific gene *goosecoid* (*gsc*), which is expressed in the Spemann's organizer, and the mesendodermal marker *notail* (*ntl*) (Figure S1J), were also normal. These markers indicate that knockdown of *pak1* did not alter CE or the formation of the dorsal-ventral axis in early zebrafish embryos.

Pak1 is highly conserved by sequence homology between humans and zebrafish, with approximately 81% sequence identity and approximately 87% sequence similarity. To determine if the function of *pak1* is conserved between species, we injected one-cell stage embryos with human *Pak1* mRNA along with the Pak1 MO directed against zebrafish *pak1*. The combined injection of the *pak1* MO and human *Pak1* mRNA caused a statistically significant rescue of injected embryos when compared to *pak1* MO alone (Figure 2A and 2B). When a kinase-dead version of human Pak1 was used, the morphant phenotype was not suppressed. Zebrafish *pak1*, but not *pak2a* or *2b*, also efficiently rescued the pak1 morphant phenotype, These data show that the biological function of *pak1* is conserved between humans and zebrafish, that these functions are not redundant with those of *pak2*, and that protein kinase activity is essential for Pak1 function in development.

Heart Defects in Pak1 Morphants

To determine the nature of the cardiovascular defects of *pak1* morphants, we performed an *in situ* hybridization using the early cardiac marker, *nkx2.5*. The expression of *nkx2.5* at 24 hpf was identical in WT and *pak1* morphant embryos, suggesting that the initial stages of cardiogenesis, including cardiomyocyte specification and initial heart tube formation, were unaffected (Figure 2A). Defects in the *pak1* morphant heart appeared by 48 hpf, when the morphant heart failed to loop (Figure 2B). Immunostaining with MF20 and S46 antibodies, marking the heart and the atrium, respectively, provided further evidence of the looping failure and also showed a defect in atrium growth (Figure 2C). In addition to the failure to loop, the *pak1* morphant heart was unable to allow blood to exit as shown in *pak1* MO-injected Tg(*Gata1:*DsRed) embryos. In *pak1* morphants, blood did not flow freely, but was seen only in the heart, suggesting an outflow blockage (Figure 2D). Sectioning through the outflow tract revealed a severe constriction (Figure 2E). *pak1* morphants did not stain with Eln2 antibodies, a marker of the bulbous arteriosis (Miao et al., 2007; Zhou et al., 2011) (Figure 2F) or the fluorescent nitric oxide indicator 4,5-diaminofluorescein diacetate (DAF-2DA) (Grimes et al., 2006) (not shown). These data suggest that *pak1* morphants have normal initial cardiogenesis, including heart tube formation, but that the heart fails to properly loop or develop the bulbous arteriosis. In these settings, blood is unable to flow and regurgitates into the atrium.

Pak1 Signaling is Crucial in Neural Crest Specification and Migration

Given the outflow tract defects we observed, we hypothesized that *pak1* morphants are defective in neural crest differentiation and migration. To test this idea, we first examined expression of *sox10* and *foxD3*, markers for undifferentiated neural crest cells, at the 16-18 somite stage. *Sox10* and *foxD3* both displayed elevated expression levels in the Pak1 morphants suggestive of a block in differentiation (Figure 2G). To examine the migration of the neural crest cells, we performed *in situ* hybridization for *crestin*. At the 16-18 somite stage, *crestin* staining shows reduced migration in the neural crest posterior to the otic placode. At the 20-somite stage, *crestin* staining displayed a loss of migration of the neural crest throughout the body and tail (Figure 2G).

Neural crest cells differentiate and become various cell and tissue types throughout the body, such as melanocytes, cartilage, and smooth muscle. By 2 dpf, the amount of melanocytes in the *pak1* morphants was significantly reduced compared to that of WT embryos (Figure 2H and 2J). Correspondingly, *mitfa*, a marker for differentiated melanophores, showed reduced staining in the *pak1* morphants (Figure 2I). Consistent with these data, the migration of melanophores was decreased in the *pak1* morphants at 2 dpf (Figure 2J and 2K). *Pak1* morphants also displayed severe abnormalities in craniofacial cartilage, including defects in Meckel's and ceratohyal cartilage and subsequent pharyngeal arches (Figure 2L). These defects were rescued by expression of zebrafish Pak1 (Figure S2). These data suggest that *pak1* is required for normal neural crest migration.

To determine if the effects of Pak1 depletion on neural crest development are cell autonomous, we injected embryos with mRNA encoding a specific peptide inhibitor of group I Paks, the Pak inhibitor domain (PID) (Zhao et al., 1998) or the negative control, PID

L107F. PID-injected, but not PID L107F injected, embryos resembled the *pak1* morphant (upper panel). We then expressed the PID in developing neural crest or heart, using the *sox10* (Dutton et al., 2008) and the *cmlc* (Huang et al., 2003) promoters, respectively. Expression of the PID, but not the inactive PID L107F, in neural crest resulted in a phenotype similar to that of the *pak1* morphant (Figure 2M, lower panels). Expression of either PID or PID L107F from the *cmlc* promoter did not visibly perturb development (Figure 2M). These data suggest that Pak1 signals primarily in the neural crest during zebrafish embryonic development.

Suppression of Pak1 Morphant Phenotype with Activated Mek

Similar to *pak1* morphants, 1-3 dpf embryos treated with CI-1040 displayed small heads, curled body axis, pericardial edema (Figure 3A and S3A). In addition, like *pak1* morphants, CI-1040 treated embryos lacked circulation (Figure 3B), suggesting that Pak1 may be signaling through the Mek/Erk pathway in cardiac development. To further test this theory, we injected a constitutively active form of Mek1 (Mek DD) along with *pak1* MO into one-cell stage embryos. Mek DD was introduced into zebrafish through a heat shock inducible system to bypass the developmental defects caused by constitutively active Mek at the one-cell stage. When induced by heat shock, virtually all cells expressed the transgene (Figure S3B). WT and with *pak1* morphant embryos were not affected by the heat shock treatment (Figure 3C). The addition of active Mek to WT embryos also caused no significant defects in development, with or without heat shock treatment (Figure 3C). *Pak1* morphants injected with Mek DD, however, displayed a significant rescue at 48 hpf upon heat shock treatment. These embryos displayed a partial rescue of body axis, less pericardial edema, and a return of circulation (Figure 3C and 3D).

We next analyzed phosphorylated Erk levels by immunohistochemistry in the *pak1* morphants at 24 hpf. Phosphorylated Erk was reduced in the head and heart region of the *pak1* morphants (Figure 3E). Interestingly, phosphorylated Erk was not uniformly reduced throughout the body of the embryo, but maintained high levels in the trunk and tail. Total phospho-Mek1 levels were also reduced in the morphants (Figure 3F).

Pak1 Signals through Gata6 in Development

A number of studies have linked Gata6 to heart formation (Kodo et al., 2009; Lepore et al., 2006; Peterkin et al., 2005; Pikkarainen et al., 2004). In zebrafish, MO knock-down of Gata6 induced a striking phenotype characterized by a lack of circulation by 3-4 dpf and formation of a non-looped heart tube (Holtzinger and Evans, 2005). Since Gata6 has previously been shown to represent an Erk target in Ras-transformed mammalian cells (Adachi et al., 2008), and the phosphorylation site in human Gata6 is conserved in the zebrafish protein, we hypothesized that Pak1 might signal through the Mek/Erk pathway to activate Gata6 in zebrafish. To evaluate this hypothesis, we first showed that Erk can phosphorylate zebrafish Gata6 *in vitro*, and that this phosphorylation is abolished if the putative phosphorylation site (Ser 265) is changed to alanine (data not shown). Next, we co-injected embryos with a *pak1* MO and an expressing vector bearing the equivalent of a constitutively phosphorylated form of Gata6 (S265D) or a non-phosphorylatable form of Gata6 (S265A). At 48 hpf, *pak1* morphants injected with Gata6 S265D appeared

significantly different from the control *pak1* morphants, with a lack of developmental defects and a return of circulation (Figure 4A-B). In comparison, embryos injected with WT Gata6 or Gata6 S265A did not show evidence of rescue, but rather retained a phenotype indistinguishable from that of control *pak1* morphants (Figure 4A-B and data not shown).

We next performed electrophoretic mobility shift assays (EMSA) to test the DNA-binding activity of Gata6. We showed that WT Gata6 was able to bind its target DNA in a dose-dependent manner (Figure 4C). We then tested the effect of phosphorylation on Gata6 DNA binding. Recombinant Gata6 was incubated in the presence or absence of Erk and ATP, then tested for activity by EMSA. We found that phosphorylated of Gata6 by Erk increased its ability to bind DNA four-fold (Figure 4D). To further test the effects of phosphorylation on Gata6 activity, HEK293 cells were transfected with WT Gata6 and a luciferase reporter plasmid containing either a promoter with a Gata6 binding element or a mutant, non-binding element (Figure 4E). WT Gata6 induced transcription of the luciferase gene about 22 times over the mutant promoter. To determine if the phosphorylation status of Ser 265 plays a role in Gata6 activation, we then introduced the Gata6 SA and SD mutants into the luciferase assay. Gata6 SD displayed three-fold more transcriptional activity than WT Gata6 or Gata6 SA (Figure 4F). These results are consistent with the idea that phosphorylation of Ser 265 activates Gata6. To further test this idea, we used Gata6 reporters to assess the effects of constitutive active Pak1 (Pak L107F) or Mek (Mek DD) on Gata6 activity. Both activated Pak1 and Mek1 significantly stimulated Gata6-responsive luciferase reporter activity over background (Figure 4G). The stimulatory effect of active Pak1 was attenuated by co-expression of Gata6 S265A (Figure 4H). These results further suggest that Erk signals through Gata6 by phosphorylating this transcription factor at Ser 265, resulting in its activation.

Discussion

Aberrant activation of Erk is associated with a number of developmental defects in vertebrate organisms (Bromberg-White et al., 2012; Sala et al., 2012; Zenker, 2011). Previous studies have shown that chemical inhibition of EGFR or Mek in zebrafish causes heart abnormalities, including pericardial edema, restricted blood flow, and an abnormal body axis (Anastasaki et al., 2012). The ability of activated Mek to suppress the *pak1* morphant phenotype is consistent with previous studies in other organisms and indicates that Pak1 acts through Mek to control development (Figure 3C). Interestingly, while *pak1* morphants display low levels of active Erk in the head and heart, phosphorylated Erk levels were not markedly reduced elsewhere in the body (Figure 3E), suggesting either a redundancy in Pak function or a different mechanism for Erk activation in the embryonic trunk and tail. This feature may account for the differences in tail morphology in *pak1* morphants versus CI-1040-treated embryos (Figure 3A).

Perhaps the most striking findings in our study are the phenotypic effects of Pak1 inhibition in the neural crest (Figure 2M) and the suppression of the *pak1* morphant phenotype by expression of an activated form of the Erk substrate Gata6 (Figure 4A). These results suggest that Gata6 activation represents a prime function for Pak1, via Erk, in zebrafish development, most likely acting in the neural crest. In this context, it is interesting to note

that Pak1 has been reported to play a role in neural crest migration in Xenopus (Bisson et al., 2012), and that Gata6 has been reported to affect cardiac neural crest migration by activating transcription of semaphorin 3C (Kodo et al., 2009; Lepore et al., 2006). In mice, Gata6 deletion in the neural crest leads to defective morphogenetic patterning of the cardiac outflow tract and aortic arch (Lepore et al., 2006). In man, mutations in *GATA6* are associated with a variety of congenital heart problems including outflow tract malformations (Kodo et al., 2009), septal defects (Wang et al., 2012), atrial fibrillation (Li et al., 2012), and tetralogy of Fallot (Huang et al., 2013). Our data suggest that Gata6 function affects development of the outflow tract as well as other neural crest derivatives in zebrafish. For example, in addition to outflow tract obstruction, *pak1* morphants displayed deranged cartilage formation and lower numbers of melanocytes, and failure of these melanocytes to migrate to their proper locations. These data imply that a Pak1 to Mek/Erk to Gata6 circuit ultimately regulates neural crest development and migration. Whether failure to activate this signaling circuit also underlies the craniofacial and cardiac abnormalities seen in *Cdc42* neural crest knockout mice remains to be determined (Liu et al., 2013).

The role of Pak1 in Erk signaling and in neural crest migration described here point to potential relationships to human disease syndromes. Defects in neural crest are associated with cardio-facio-cutaneous syndromes, such as Noonan's, Costello, and LEOPARD syndrome. Interestingly, germ-line mutations that result in constitutive Erk activation cause many of these overlapping developmental syndromes, sometimes termed Rasopathies (Anastasaki et al., 2012). These abnormal developmental syndromes have several features in common, including heart defects, skin abnormalities, and distinctive facial features. How Erk overactivation leads to these phenotypes is not known, though, in a zebrafish model of LEOPARD syndrome, it has been suggested that downregulation of *foxd3* and *sox10* by Erk is important for normal neural crest migration, with subsequent effects on development (Stewart et al., 2010). Here, we suggest that Gata6 activation by Erk plays a central role in the zebrafish development related to neural crest migration. For these reasons, the characterization of a Pak-Mek-Erk-Gata6 signaling module not only helps clarify an important developmental molecular pathway, but also may point to potential new therapeutic targets in Rasopathy syndromes.

EXPERIMENTAL PROCUDURES

Zebrafish Stocks and Embryo Collection

Wild-type AB and transgenic zebrafish lines were maintained in the Zebrafish Core Facility of the Fox Chase Cancer Center under standard conditions (Kimmel et al., 1995). Embryo collection and maintenance were carried out as previously described (Rhodes et al., 2009).

MO Design and Analysis

The *pak1* MO (GeneTools, LLC, Philomath, OR) was designed to target the *pak1* exon1-intron1 boundary (5'- GCATCACTCACTCTTGTCTCCTC-3'). Embryos were injected as previously described (Lightcap et al., 2009). Effects on zebrafish *pak1* (accession number NM_201328) splicing was analyzed by RT-PCR using the One Step RT-PCR kit (Qiagen) Primers were designed to bind to the first exon (forward) and the second exon (reverse) of

zebrafish *pak1*: 5’ ACTGGGATCCATGTCAGACAATGGGGAGTAGAG 3’ and 5’ CGTCTGGAGTAATCGAGCCCACTGCTCAGGCAT 3’. Cyclophilin was used as a loading control. *pak1* ATG MO, *pak2a* and *pak2b* MO were designed as previously published (Buchner et al., 2007; Lightcap et al., 2009). Unless otherwise indicated, MOs were used at 1.49 ng/embryo, and n numbers represent the total from three batches of embryos, performed and analyzed independently.

Immunoblot Analysis

Zebrafish embryos were collected at noted time points and deyolked as previously described (Link et al., 2006). Membranes were blocked with 5% BSA overnight and probed using the SNAP i.d.® System (Millipore). Membranes were incubated with 1:1000 Pak1 antibodies (1:1000) for 15 minutes. Membranes were washed with TBST and incubated with HRP conjugated antibodies (1:10,000).

Zebrafish Rescue Experiments

Human *PAK1* cDNA was subcloned into *Bam*HI and *Eco*RI sites of the pCS2 vector. Human transcripts were transcribed *in vitro* using the mMessage Machine kit (Ambion). RNAs were injected into 1-cell stage zebrafish embryos as described previously (Lightcap et al., 2009). Mek-DD (S219D, S223D) and Gata6 (S265A or S265D) were subcloned into pSGH2 vector. The plasmid was co-injected at 5 ng/μL with 1 mM *pak1* MO into AB embryos at the 1-cell stage. At 24 hpf, the fish were heat shocked at 38°C for 1 hr to induce the expression of the protein of interest and GFP. Embryos were examined 2 hours after heat shock to determine the expression of GFP. At 48 hpf, embryos were examined for rescue of the phenotype. PID or PID L107F expression driven by the *sox10* or *cmlc* promoters were injected into 1-cell stage embryos a concentration of 30 ng/μL. At 48 hpf, the embryos were examined for phenotypes.

Sectioning and Staining

AB embryos were injected with the *pak1* MO at the 1-cell stage. At 48 hpf, the embryos were fixed in 4% paraformaldehyde. The embryos were then frozen in OCT compound and cut into 12 μm transverse sections. Sections were stained with H&E for visualization. Eln2 antibodies were used to visualize the bulbous arteriosis (Zhou et al., 2011). DAF-2DA staining was performed as previously published (Grimes et al., 2006).

Imaging

Dechorionated embryos were placed on a glass depression slide in 1% methylcellose and morphology was assessed visually using a light transmission Nikon SMZ 1500. Representative images were recorded using a Nikon digital sight DS Fi1 camera.

Whole-Mount *in-situ* Hybridization, Immunohistochemistry, and Cartilage Staining

Whole-mount *in-situ* hybridization and immunohistochemistry was performed as previously described (Bolli et al., 2011; Koshida et al., 2005; Yelon et al., 1999). p-Erk (Cell Signaling #9101) was used as primary antibody and DAB was used for visualization. Cartilage staining was preformed as previously described (Kimmel et al., 1998).

Luciferase and EMSA Assays

Assays were performed by manufacturer's protocols, using Promega, Dual-Glo Luciferase Assay System, and Molecular Probes, EMSA Kit E33075, respectively. For EMSA assays, the oligonucleotide contained a Gata6 site (5'-CAA AGG GCC GAT GGG CAG ATA GAG GAG AGA CAG GA-3') (Molkentin et al., 1994). Luciferase assays were carried out using Gata6 reporter constructs (Kodo et al., 2009).

Supplementary Material

Refer to Web version on PubMed Central for supplementary material.

Acknowledgments

We thank Hiroyoki Yamagashi for Gata6 reporter plasmids, Qing Jing for zPak1 antibodies, Geoffrey Burns for Eln2 antibodies, Rebecca Burdine for the Tg(*cmlc2*:EGFP) line, David Wiest for the pSGH2 vector and *bmp4* and *ntl* probes, and Thomas Shilling, Thomas Look, Igor Dawid, and Jeroen den Hertog for providing probes for *foxd3, crestin*, *mitfa, dlx3*, and *hgg1*, respectively. We also thank the Fox Chase Cancer Center Zebrafish Facility for enabling this project and the Fox Chase Cancer Center Pathology department for their assistance. This work was supported by grants from the NIH to JC (R01 CA58836 and R01 CA098830) and to the Fox Chase Cancer Center (P30 CA006927), as well as by an appropriation from the state of Pennsylvania.

References

Adachi Y, Shibai Y, Mitsushita J, Shang WH, Hirose K, Kamata T. Oncogenic Ras upregulates NADPH oxidase 1 gene expression through MEK-ERK-dependent phosphorylation of GATA-6. Oncogene. 2008; 27:4921–4932. [PubMed: 18454176]

Anastasaki C, Rauen KA, Patton EE. Continual low-level MEK inhibition ameliorates cardio-facio-cutaneous phenotypes in zebrafish. Dis Model Mech. 2012; 5:546–552. [PubMed: 22301711]

Arias-Romero LE, Chernoff J. A tale of two Paks. Biol Cell. 2008; 100:97–108. [PubMed: 18199048]

Bisson N, Wedlich D, Moss T. The p21-activated kinase Pak1 regulates induction and migration of the neural crest in Xenopus. Cell cycle. 2012; 11:1316–1324. [PubMed: 22421159]

Bokoch GM. Biology of the p21-activated kinases. Annu Rev Biochem. 2003; 72:743–781. [PubMed: 12676796]

Bolcome RE 3rd, Chan J. Constitutive MEK1 activation rescues anthrax lethal toxin-induced vascular effects in vivo. Infect Immun. 2010; 78:5043–5053. [PubMed: 20855511]

Bolli N, Payne EM, Rhodes J, Gjini E, Johnston AB, Guo F, Lee JS, Stewart RA, Kanki JP, Chen AT, et al. cpsf1 is required for definitive HSC survival in zebrafish. Blood. 2011; 117:3996–4007. [PubMed: 21330472]

Bromberg-White JL, Andersen NJ, Duesbery NS. MEK genomics in development and disease. Brief Funct Genomics. 2012; 11:300–310. [PubMed: 22753777]

Buchner DA, Su F, Yamaoka JS, Kamei M, Shavit JA, Barthel LK, McGee B, Amigo JD, Kim S, Hanosh AW, et al. pak2a mutations cause cerebral hemorrhage in redhead zebrafish. Proc Natl Acad Sci U S A. 2007; 104:3996–4001. [PubMed: 17360466]

Chow HY, Jubb AM, Koch JN, Jaffer ZM, Stepanova D, Campbell DA, Duron SG, O'Farrell M, Cai KQ, Klein-Szanto AJ, et al. p21-Activated kinase 1 is required for efficient tumor formation and progression in a Ras-mediated skin cancer model. Cancer Res. 2012; 72:5966–5975. [PubMed: 22983922]

Dummler B, Ohshiro K, Kumar R, Field J. Pak protein kinases and their role in cancer. Cancer metastasis reviews. 2009; 28:51–63. [PubMed: 19165420]

Dutton JR, Antonellis A, Carney TJ, Rodrigues FS, Pavan WJ, Ward A, Kelsh RN. An evolutionarily conserved intronic region controls the spatiotemporal expression of the transcription factor Sox10. BMC developmental biology. 2008; 8:105. [PubMed: 18950534]

Grimes AC, Stadt HA, Shepherd IT, Kirby ML. Solving an enigma: arterial pole development in the zebrafish heart. Dev Biol. 2006; 290:265–276. [PubMed: 16405941]

Higuchi M, Onishi K, Kikuchi C, Gotoh Y. Scaffolding function of PAK in the PDK1-Akt pathway. Nat Cell Biol. 2008; 10:1356–1364. [PubMed: 18931661]

Holtzinger A, Evans T. Gata4 regulates the formation of multiple organs. Development. 2005; 132:4005–4014. [PubMed: 16079152]

Huang CJ, Tu CT, Hsiao CD, Hsieh FJ, Tsai HJ. Germ-line transmission of a myocardium-specific GFP transgene reveals critical regulatory elements in the cardiac myosin light chain 2 promoter of zebrafish. Dev Dyn. 2003; 228:30–40. [PubMed: 12950077]

Huang RT, Xue S, Xu YJ, Yang YQ. Somatic mutations in the GATA6 gene underlie sporadic tetralogy of Fallot. Int J Mol Med. 2013; 31:51–58. [PubMed: 23175051]

Jopling C, van Geemen D, den Hertog J. Shp2 knockdown and Noonan/LEOPARD mutant Shp2-induced gastrulation defects. PLoS Genet. 2007; 3:e225. [PubMed: 18159945]

Kimmel CB, Ballard WW, Kimmel SR, Ullmann B, Schilling TF. Stages of embryonic development of the zebrafish. Dev Dyn. 1995; 203:253–310. [PubMed: 8589427]

Kimmel CB, Miller CT, Kruze G, Ullmann B, BreMiller RA, Larison KD, Snyder HC. The shaping of pharyngeal cartilages during early development of the zebrafish. Dev Biol. 1998; 203:245–263. [PubMed: 9808777]

Kodo K, Nishizawa T, Furutani M, Arai S, Yamamura E, Joo K, Takahashi T, Matsuoka R, Yamagishi H. GATA6 mutations cause human cardiac outflow tract defects by disrupting semaphorin-plexin signaling. Proc Natl Acad Sci U S A. 2009; 106:13933–13938. [PubMed: 19666519]

Koshida S, Kishimoto Y, Ustumi H, Shimizu T, Furutani-Seiki M, Kondoh H, Takada S. Integrinalpha5-dependent fibronectin accumulation for maintenance of somite boundaries in zebrafish embryos. Dev Cell. 2005; 8:587–598. [PubMed: 15809040]

Krens SF, He S, Lamers GE, Meijer AH, Bakkers J, Schmidt T, Spaink HP, Snaar-Jagalska BE. Distinct functions for ERK1 and ERK2 in cell migration processes during zebrafish gastrulation. Dev Biol. 2008; 319:370–383. [PubMed: 18514184]

Lepore JJ, Mericko PA, Cheng L, Lu MM, Morrisey EE, Parmacek MS. GATA-6 regulates semaphorin 3C and is required in cardiac neural crest for cardiovascular morphogenesis. J Clin Invest. 2006; 116:929–939. [PubMed: 16557299]

Li J, Liu WD, Yang ZL, Yang YQ. Novel GATA6 loss-of-function mutation responsible for familial atrial fibrillation. Int J Mol Med. 2012; 30:783–790. [PubMed: 22824924]

Lightcap CM, Kari G, Arias-Romero LE, Chernoff J, Rodeck U, Williams JC. Interaction with LC8 is required for Pak1 nuclear import and is indispensable for zebrafish development. PLoS One. 2009; 4:e6025. [PubMed: 19557173]

Link V, Shevchenko A, Heisenberg CP. Proteomics of early zebrafish embryos. BMC Dev Biol. 2006; 6:1. [PubMed: 16412219]

Liu Y, Jin Y, Li J, Seto E, Kuo E, Yu W, Schwartz RJ, Blazo M, Zhang SL, Peng X. Inactivation of Cdc42 in neural crest cells causes craniofacial and cardiovascular morphogenesis defects. Dev Biol. 2013; 383:239–252. [PubMed: 24056078]

Miao M, Bruce AE, Bhanji T, Davis EC, Keeley FW. Differential expression of two tropoelastin genes in zebrafish. Matrix biology : journal of the International Society for Matrix Biology. 2007; 26:115–124. [PubMed: 17112714]

Molkentin JD, Kalvakolanu DV, Markham BE. Transcription factor GATA-4 regulates cardiac muscle-specific expression of the alpha-myosin heavy-chain gene. Mol Cell Biol. 1994; 14:4947–4957. [PubMed: 8007990]

Peterkin T, Gibson A, Loose M, Patient R. The roles of GATA-4, -5 and -6 in vertebrate heart development. Semin Cell Dev Biol. 2005; 16:83–94. [PubMed: 15659343]

Pikkarainen S, Tokola H, Kerkela R, Ruskoaho H. GATA transcription factors in the developing and adult heart. Cardiovasc Res. 2004; 63:196–207. [PubMed: 15249177]

Razzaque MA, Komoike Y, Nishizawa T, Inai K, Furutani M, Higashinakagawa T, Matsuoka R. Characterization of a novel KRAS mutation identified in Noonan syndrome. Am J Med Genet A. 2012; 158A:524–532. [PubMed: 22302539]

Rhodes J, Amsterdam A, Sanda T, Moreau LA, McKenna K, Heinrichs S, Ganem NJ, Ho KW, Neuberg DS, Johnston A, et al. Emi1 maintains genomic integrity during zebrafish embryogenesis and cooperates with p53 in tumor suppression. Mol Cell Biol. 2009; 29:5911–5922. [PubMed: 19704007]

Runtuwene V, van Eekelen M, Overvoorde J, Rehmann H, Yntema HG, Nillesen WM, van Haeringen A, van der Burgt I, Burgering B, den Hertog J. Noonan syndrome gain-of-function mutations in NRAS cause zebrafish gastrulation defects. Dis Model Mech. 2011; 4:393–399. [PubMed: 21263000]

Sala V, Gallo S, Leo C, Gatti S, Gelb BD, Crepaldi T. Signaling to cardiac hypertrophy: insights from human and mouse RASopathies. Mol Med. 2012; 18:938–947. [PubMed: 22576369]

Stewart RA, Sanda T, Widlund HR, Zhu S, Swanson KD, Hurley AD, Bentires-Alj M, Fisher DE, Kontaridis MI, Look AT, Neel BG. Phosphatase-dependent and -independent functions of Shp2 in neural crest cells underlie LEOPARD syndrome pathogenesis. Dev Cell. 2010; 18:750–762. [PubMed: 20493809]

Wang J, Luo XJ, Xin YF, Liu Y, Liu ZM, Wang Q, Li RG, Fang WY, Wang XZ, Yang YQ. Novel GATA6 mutations associated with congenital ventricular septal defect or tetralogy of fallot. DNA Cell Biol. 2012; 31:1610–1617. [PubMed: 23020118]

Yelon D, Horne SA, Stainier DY. Restricted expression of cardiac myosin genes reveals regulated aspects of heart tube assembly in zebrafish. Dev Biol. 1999; 214:23–37. [PubMed: 10491254]

Zenker M. Clinical manifestations of mutations in RAS and related intracellular signal transduction factors. Curr Opin Pediatr. 2011; 23:443–451. [PubMed: 21750428]

Zhao ZS, Manser E, Chen XQ, Chong C, Leung T, Lim L. A conserved negative regulatory region in alphaPAK: inhibition of PAK kinases reveals their morphological roles downstream of Cdc42 and Rac1. Mol Cell Biol. 1998; 18:2153–2163. [PubMed: 9528787]

Zhou Y, Cashman TJ, Nevis KR, Obregon P, Carney SA, Liu Y, Gu A, Mosimann C, Sondalle S, Peterson RE, et al. Latent TGF-beta binding protein 3 identifies a second heart field in zebrafish. Nature. 2011; 474:645–648. [PubMed: 21623370]

Highlights

- Pak1 is required for the activation of Erk in the central nervous system and heart
- Active Erk phosphoryates and activates the transcription factor Gata6
- Expression of activated Mek1 or Gata6 is sufficient to compensate for loss of Pak1
- A Pak1/Erk/Gata6 signaling module regulates neural crest migration

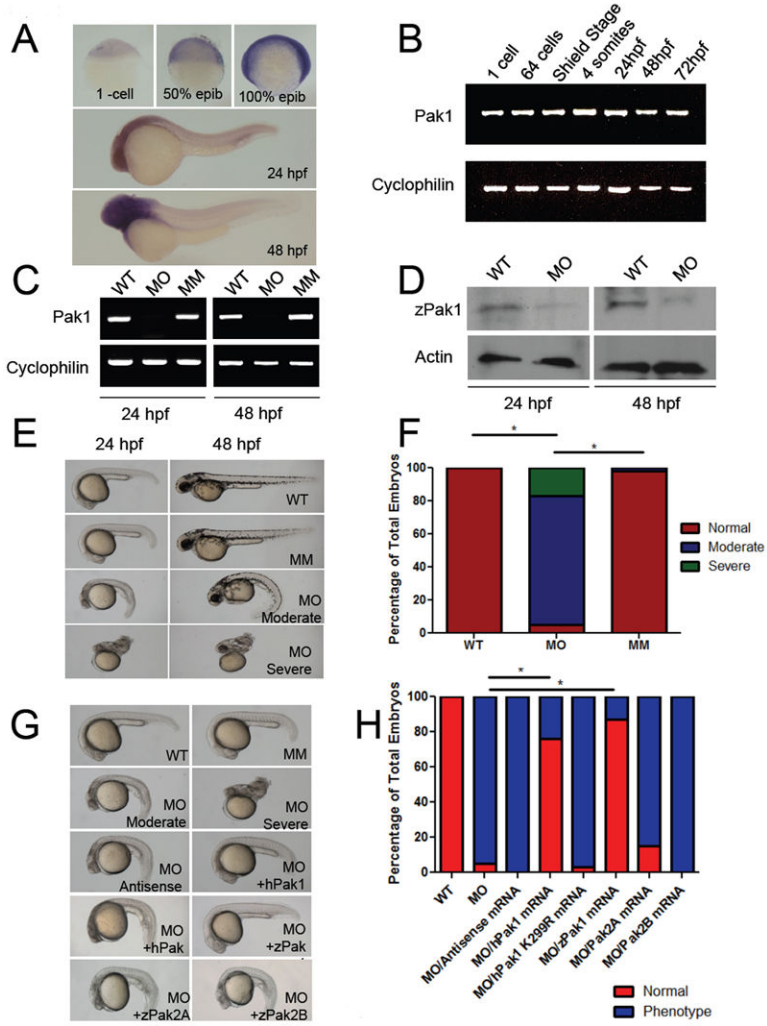

Figure 1. Pak1 is required for normal development of zebrafish

(A) Transcripts for *pak1* were detected by whole mount in situ hybridization at the stages indicated. Hours post fertilization (hpf). (B) Expression of *pak1* at various stages in development by RT-PCR. (C) RT-PCR analysis of *pak1* transcripts in morphants compared to WT and mismatch MO injected embryos at 24 and 48 hpf. (D) Immunoblot analysis of Pak1 in morphants compared to WT at 24 and 48 hpf. (E) Representative images of the moderate (MO moderate) and severe (MO severe) *pak1* knockdown phenotypes as compared to the wild-type (WT) and mismatch morpholino (MM) injected embryos at 24 hpf and 48 hpf. (F) Quantification of *pak1* knockdown phenotype at 24 hpf. (G) Morphology of embryos injected with the indicated MOs plus mRNA for wild-type of kinase-dead human Pak1 (hPak1), wild-type zebrafish Pak1 (zPak1), zPak2a, or zPak2b. (H) Quantitation of phenotypes at 24 hpf. * $p<0.0001$. (G) *In situ* hybridization for *sox10* and *foxD3* at 16-18 somites (lateral and cranial views). Arrows point to cranial neural crest expression in lateral view. *In situ* hybridization for *crestin* at the 16-18 and the 20 somite stage. Note lack of migration of neural crest in cranial view (arrows) and down the tail in the lateral view. (H) Trunk images of *pak1* morphants lacking melanophores at 2 dpf. (I) *In situ* hybridization for *mitfa.* (J) Quantification of melanophores at 2 dpf. (K) Quantification of

melanophores migration in *pak1* morphants compared to mismatch MO injected embryos. (L) Cartilage staining (Alcian Blue) at 6 dpf. (M) (upper panel) WT embryos were injected with either PID (Pak inhibitor) or PID L107F (inactive Pak inhibitor) mRNA. Embryos are shown at 48 hpf; (lower panel) WT embryos were injected with expression vectors encoding PID or PID L107F driven by the *sox10* promoter or the *cmlc* promoter, as indicated. Images were taken at 48 hpf.

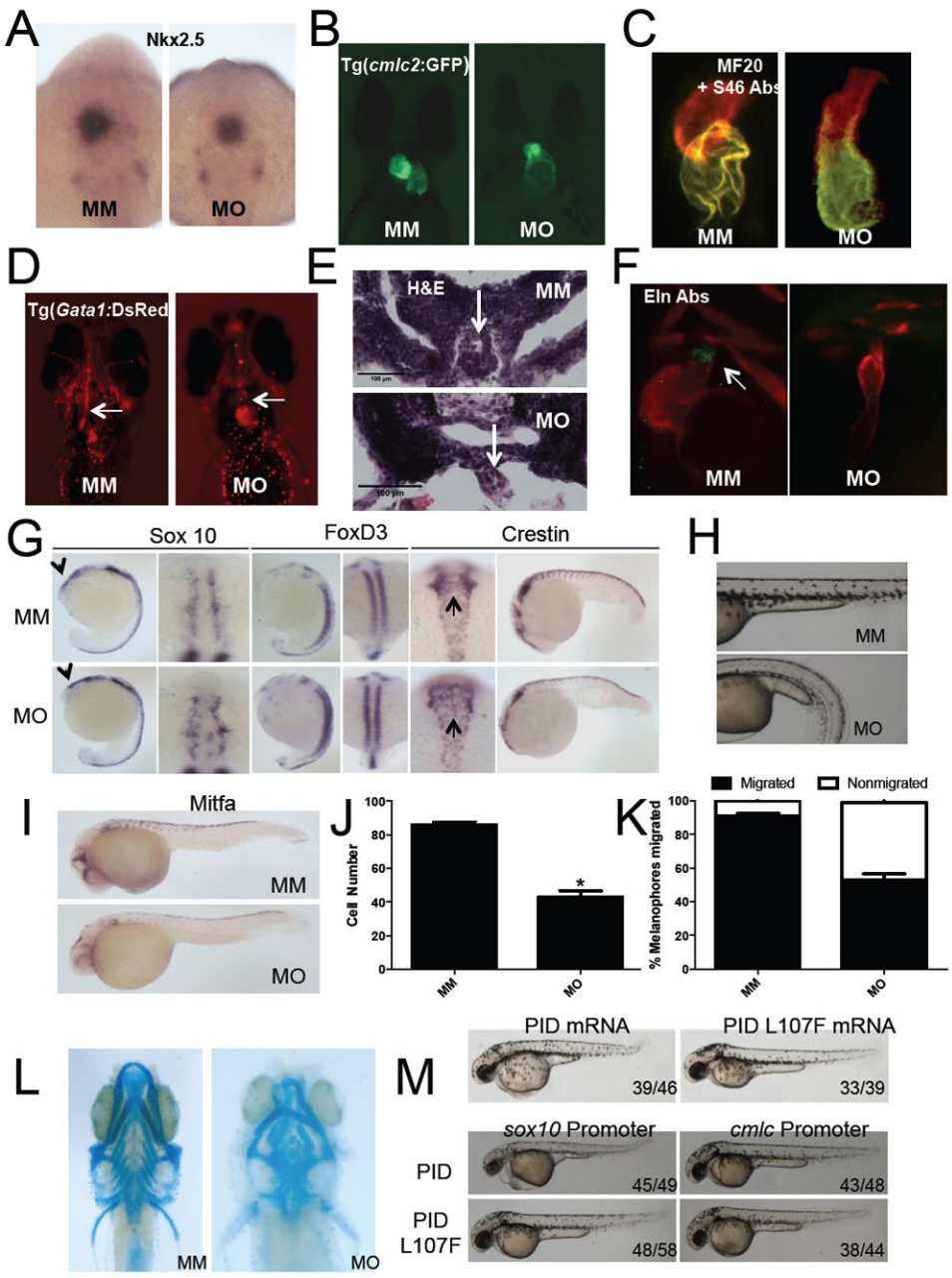

Figure 2. Pak1 morphants display cardiac and neural crest defects

(A) Transcript expression of *nkx2.5* shown by *in situ* hybridization at 20 somites. (B-C) *Pak1* morphant heart does not loop at 48 hpf as shown by Tg(*cmlc2*:GFP) immunofluorescence and staining with MF20 and S46 antibodies. (D) Ventral images of 48 hpf Tg(*Gata1:*DsRed) show a cardiac outflow tract blockage with no blood flow throughout the head vasculature in the *pak1* morphants (MO) compared to MM embryos (MM). Arrows point to cardiac outflow tract. (E) Transverse sections of the cardiac outflow tract in MO and MM injected embryos stained with H&E. Arrows point to the cardiac outflow tract. (F) Eln2 staining of WT and *pak1* morphant embryos. Arrow indicates region of Eln positivity.

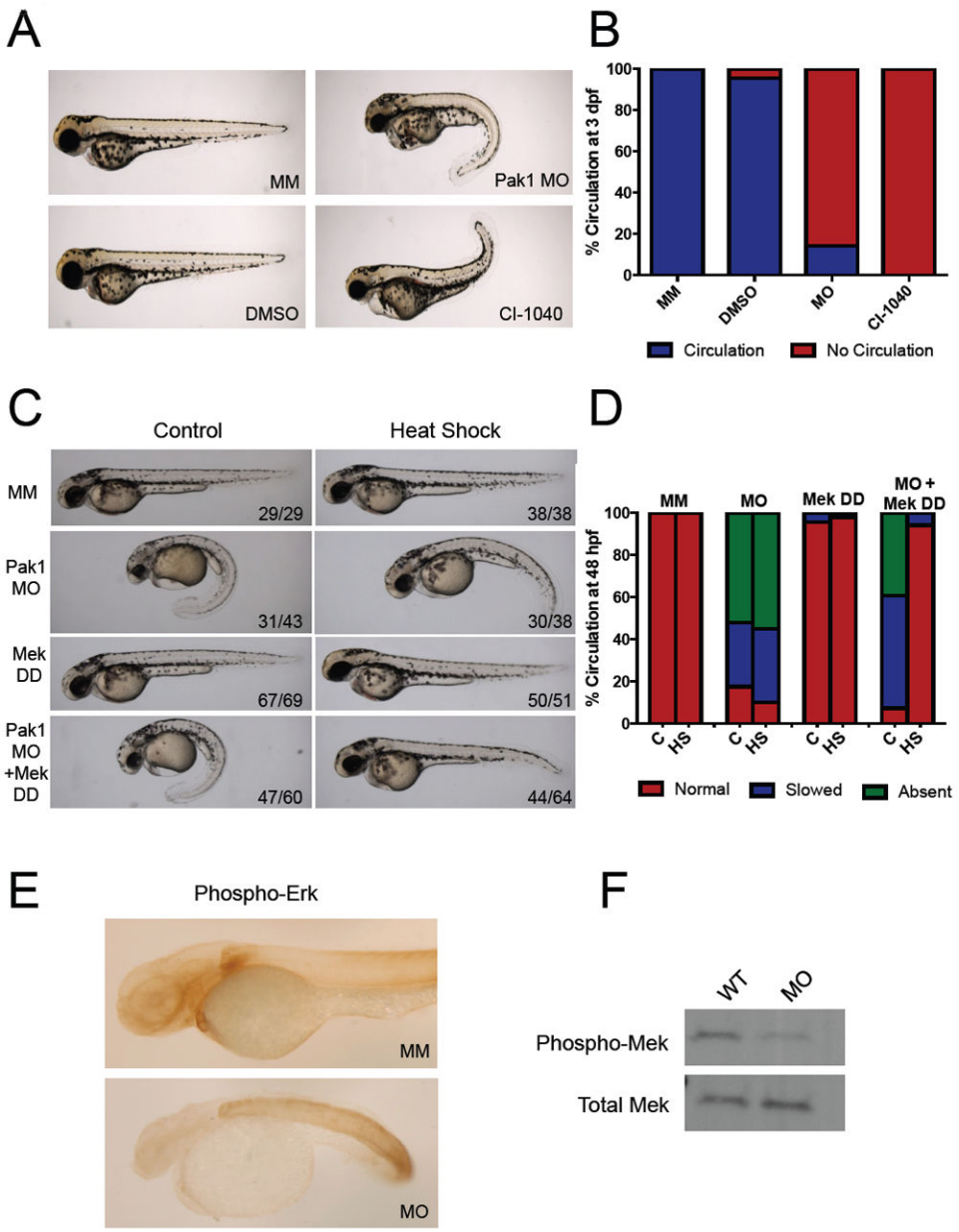

Figure 3. Pak1 signals through the Erk pathway in heart development

(A) Comparison of chemical inhibition of Mek and *pak1* morphants at 3 dpf. WT embryos were placed in egg water containing DMSO or 1 μM CI-1040 at the 1-cell stage. The water was changed every 24 hours with new drug. The embryos were analyzed for gross morphology and presence or absence of circulation. (B) Quantification of circulation seen with Mek inhibition at 48 hpf. (C) Representative images of 48 hpf *pak1* morphants rescued by an active form of Mek (Mek DD). An inducible Mek1 DD expression plasmid was coinjected with the *pak1* MO at the one-cell stage, followed by heat-shock at 24 hpf as indicated. (D) Immunohistochemistry for phosphorylated Erk.

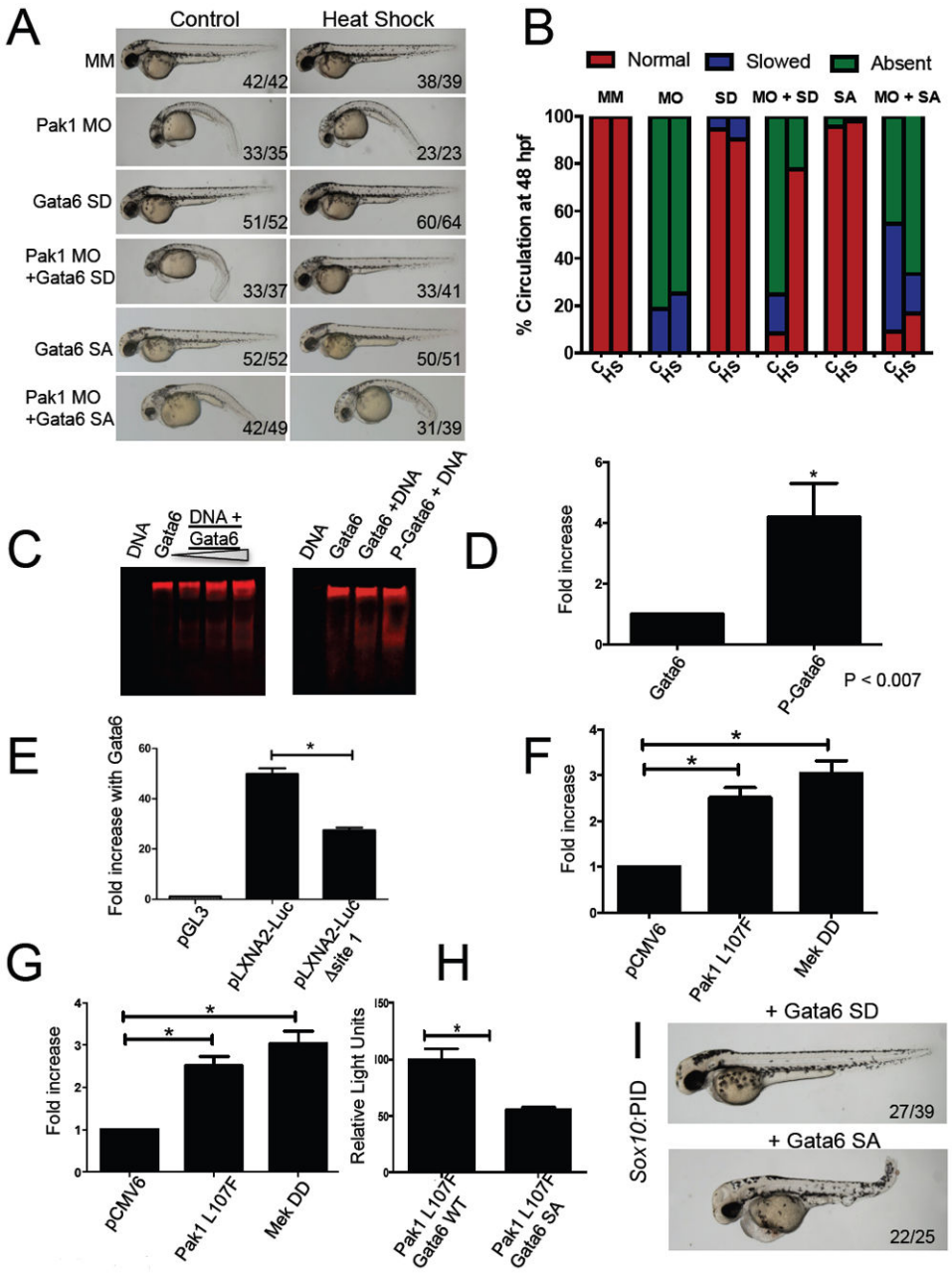

Figure 4. Active Gata6 can compensate for loss of Pak1

(A) Representative images of *pak1* morphants that have been rescued by the addition of an active form of Gata6 (Gata6 SD) but not by the inactive mutant (Gata6 SA). (B) Quantification of circulation in the Gata6 rescue. The indicated inducible Gata6 expression plasmids were coinjected with *pak1* MO at the 1-cell stage, followed by heat-shock at 24 hpf as indicated. (C) Dose-dependent binding of WT Gata6 to a GATA-containing DNA template (EMSA assay). (D) Fluorescent EMSA showing that Gata6 when phosphorylated by ERK is able to bind to target DNA more efficiently than unphosphorylated Gata6. (E) Luciferase Assay showing that WT Gata6 is able to bind WT target DNA and promote transcription. This activity is lost however when the Gata6 binding site on the promoter is

mutated. (F) Luciferase assays, comparing Gata6 SD to WT or Gata6 SA; (G) comparing active Pak1 (Pak L107F) and MEK DD, respectively, to control; and (H) comparing activated Pak1 plus either Gata6 WT or Gata6 SA. (I) WT embryos were injected with a vector encoding PID driven by the *sox10* promoter plus an expression vector encoding either Gata6 SD or SA. Representative images were taken at 48 hpf.